Vibrational self-consistent field approach to anharmonic spectroscopy of molecules in solids: Application to iodine in argon matrix

Z. Bihary
Department of Chemistry, University of California, Irvine, California 92697

R. B. Gerber
The Hebrew University, Jerusalem 91904, Israel, and Department of Chemistry, University of California, Irvine, California 92697

V. A. Apkarian
Department of Chemistry, University of California, Irvine, California 92697

(Received 7 February 2001; accepted 18 May 2001)

An extension of the vibrational self-consistent field (VSCF) method is developed for quantitative calculations of molecular vibrational spectroscopy in a crystalline solid environment. The approach is applicable to fields such as matrix-isolation spectroscopy and spectroscopy of molecular crystals. Advantages of the method are that extended solid vibrations and their coupling to intramolecular modes are incorporated, and that the treatment includes anharmonic effects, both due to the intrinsic property of individual modes and due to coupling between modes. Suitable boundary conditions are adopted in treating the solid environment. In applications, e.g., molecules in rare-gas crystals, hundreds of coupled molecular and matrix modes can be handled computationally. The method is applied to the vibrational matrix-shift of iodine in an argon matrix, and the calculated overtone frequencies are compared to experimental values obtained from both time-domain coherent Raman and frequency-domain Resonance Raman measurements. The physical origin of the shifts is interpreted in detail, and the properties of the iodine–argon interactions essential to obtain the correct sign and magnitude of the shift are elucidated. An I_2–Ar potential, based on anisotropic atom–atom interactions and fitted to *ab initio* calculations, gives the best agreement with experiment. The results show that the VSCF solid-state approach is a powerful tool for matrix spectroscopy. © *2001 American Institute of Physics.* [DOI: 10.1063/1.1384870]

I. INTRODUCTION

Vibrational spectroscopy methods are among the most important tools in the molecular sciences. One of the frontiers is high resolution spectroscopy in condensed phases. There is, for example, a growing number of accurate spectroscopic measurements by a variety of new or improved methods on molecules in a solid environment. Spectroscopy of molecular species isolated in rare-gas matrices, a subject pioneered by Pimentel and co-workers,[1] is one of the disciplines where high-resolution data is often obtained, and where it can have important applications.[2–4] In cases where sharp vibrational lines are observed, tools of quantitative interpretation are obviously desirable. Successful calculations and comparison with experiment can then provide very useful insight on the intramolecular force field of the trapped species, and also on the interaction between the molecule and the surrounding atoms.[5] The challenge of such a treatment is, however, a formidable one, since the solution for the vibrational states of a many-atom system is required. This can be done in a straightforward way only in the harmonic approximation. However, for most purposes such a treatment is inadequate, in some cases dramatically so, such as for floppy molecules, hydrogen-bonded complexes in the matrix, etc. Even in cases where anharmonicity is very modest, the accuracy of the available data justifies going beyond the harmonic level.[6] The treatment of matrix effects on the molecular vibrational lines would have been relatively simple, of course, had the media been of static atoms. In fact, both theoretical considerations and ample experimental evidence show that the dynamics of the matrix vibrations often plays an important role.[7] Even when the observed transitions can be assigned in terms of the modes of the free molecule, lattice dynamics is often significantly coupled to the molecular vibrations, and must be incorporated in a general quantitative treatment.

The objective of the present paper is to develop a general, quantitative algorithm for calculations of vibrational spectroscopy of molecules in matrices. The treatment that will be pursued is at the anharmonic level, and interactions between different modes are treated, though approximately. Dynamical effects due to lattice vibrations, as well as the static effects of the matrix atoms, are included. At the basis of our treatment is the vibrational self-consistent field (VSCF) method, which has been extensively used for polyatomic molecules, including very large ones, in recent years.[8] In essence, the present study extends the VSCF method to molecules in matrices, and applies appropriate boundary conditions for the system. The good scaling property of VSCF with system size allows us to explicitly include many vibrational modes of the matrix as well as those of the embedded molecule.

We chose to first test the method for iodine in argon

matrices. Accurate overtone data is available for this system from frequency-domain Resonance Raman (RR) spectra[9,10] and time-domain coherent Raman scattering (CARS) measurements.[11] The observed matrix shifts are very small, but this is an interesting challenge in its own right: The study will explore whether the method has sufficient accuracy to analyze the shifts, and whether it can be used to determine a good potential for I_2 in argon.

The structure of the paper is as follows. In Sec. II, we review the vibrational self-consistent field method, and describe its application to extended systems. We describe the adopted boundary condition and discuss its advantage for the present application. Section III outlines the model of the system, and introduces the potential functions tested. The results are presented and analyzed in Sec. IV. Concluding remarks are brought in Sec. V.

II. METHOD

A. Vibrational self-consistent field (VSCF) method

It will be useful to give here a brief outline of the VSCF method for polyatomic systems[8] and to discuss later the necessary adaptation of the algorithm for the study of molecular spectroscopy in solids. For a given equilibrium geometry of a system, normal-mode analysis yields harmonic frequencies and normal mode coordinates. The vibrational Schroedinger equation in mass-weighted normal coordinates $Q_1,\ldots,Q_N$ is given as

$$\left(-\frac{1}{2}\sum_{j=1}^{N}\frac{\partial^2}{\partial Q_j^2}+V(Q_1,\ldots,Q_N)\right)\psi_n(Q_1,\ldots,Q_N) = E_n\psi_n(Q_1,\ldots,Q_N), \tag{1}$$

where $V(Q_1,\ldots,Q_N)$ is the full potential and N is the number of vibrational degrees of freedom. The VSCF approximation uses the separability ansatz,

$$\psi_n(Q_1,\ldots,Q_N)=\prod_{j=1}^{N}\psi_j^{(n)}(Q_j), \tag{2}$$

which leads to the single-mode VSCF equations

$$\left(-\frac{1}{2}\frac{\partial^2}{\partial Q_j^2}+\overline{V}_j^{(n)}(Q_j)\right)\psi_j^{(n)}=\epsilon_n\psi_j^{(n)}, \tag{3}$$

where the effective VSCF potential $\overline{V}_j^{(n)}(Q_j)$ for mode Q_j is

$$\overline{V}_j^{(n)}(Q_j)=\left\langle\prod_{l\neq j}^{N}\psi_l^{(n)}(Q_l)\middle|V(Q_1,\ldots,Q_N)\times\middle|\prod_{l\neq j}^{N}\psi_l^{(n)}(Q_l)\right\rangle. \tag{4}$$

Equations (3) and (4) are solved self-consistently, giving the set of VSCF single-mode energies and single-mode wave functions. The total VSCF energy is given by

$$E_n^{\mathrm{VSCF}}=\sum_{j=1}^{N}\epsilon_j^{(n)}-(N-1)\left\langle\prod_{j=1}^{N}\psi_j^{(n)}(Q_j)\middle|\times V(Q_1,\ldots,Q_N)\middle|\prod_{j=1}^{N}\psi_j^{(n)}(Q_j)\right\rangle. \tag{5}$$

After obtaining the VSCF solution, it can be corrected for correlation effects using second-order perturbation theory.[12] For the system studied later as application, the correlation corrections beyond VSCF are extremely small. However, should it be necessary in other systems to do so, the perturbation theoretic corrections to VSCF are simple enough to be included in solid spectroscopic calculations.

The main computational difficulty of the above scheme is the evaluation of the multidimensional integrals in Eqs. (4)–(5), which contain the full potential $V(Q_1,\ldots,Q_N)$. Different schemes have been proposed to overcome this difficulty. For the present application that deals with a great number of modes, the most suitable solution is the approximation of pairwise mode interactions. This simplifies potential V as follows:

$$V(Q_1,\ldots,Q_N)=\sum_{j}^{N}V_j^{\mathrm{diag}}(Q_j)+\sum_{i}\sum_{i<j}V_{ij}^{\mathrm{coup}}(Q_i,Q_j), \tag{6}$$

where $V_j^{\mathrm{diag}}(Q_j)=V(0,...,Q_j,\ldots,0)$ are the "diagonal," single-mode terms and $V_{ij}^{\mathrm{coup}}(Q_i,Q_j)=V(0,...,Q_j,\ldots,Q_i,\ldots,0)$ are the pairwise mode–mode coupling terms. Couplings between three and more normal modes are neglected. This approximation of pair-wise interactions has been shown to work reasonably well for many systems with empirical potentials,[13,14] as well as in studies of clusters of moderate size, using *ab initio* potentials.[15] In any case, this approximation is an assumption that must be checked in each application. Within the pair-wise approximation, the calculation of effective VSCF potentials (4) involves only 1-D integrals of the form

$$V_j^{\mathrm{coup},n}(Q_j)=\langle\psi_i(Q_i)|V_{ij}^{\mathrm{coup}}|\psi_i(Q_i)\rangle, \tag{7}$$

and the calculation of the total VSCF energies requires up to 2-D integrals. The computation of these integrals is done numerically, using a grid representation of single-mode and pair-coupling potentials. The single-mode VSCF equations (3) are also solved numerically using the sinc-DVR method.[16] The grid points for each normal mode coordinate Q_i are chosen equidistantly on an interval $[-Q_{\max},Q_{\max}]$, where $Q_{\max}$ is proportional to $\omega_i^{-1/2}$, i.e., to the zero-point amplitude of mode *i*. The number of grid points necessary for accurate calculation depends on the number of relevant eigenstates for each mode.[17] Typically 8-point grids are sufficient if only the ground-state and the first excited state are of interest. For higher excited states, more grid points and larger intervals are necessary.

While VSCF was first developed in the context of two-mode systems,[18] the method was found to scale very favorably with system size. Algorithms were developed that are particularly useful for large systems.[19] The number of coupled modes that can be efficiently treated depends on the level of theory used for calculating the potential energy sur-

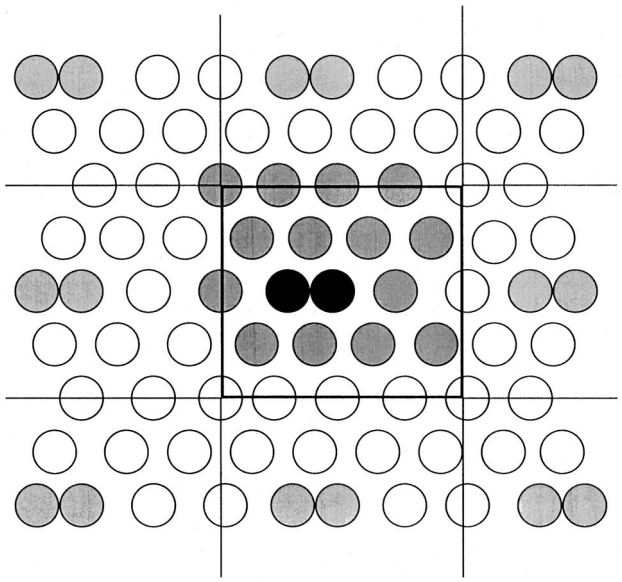

FIG. 1. Schematic picture of the simulation cell and its effective repetitions for Periodic Boundary Conditions.

face. State-of-the-art *ab initio* calculations have recently been performed on the glycine molecule (18 coupled modes).[15] If empirical potentials with simple analytic forms are used, calculations on systems with hundreds, or even thousands of modes become feasible, while retaining the inherently anharmonic and quantum natures of the method. This good scaling property allows us to extend VSCF to the study of solids, such as matrix-isolated molecules considered in the present application.

B. Boundary conditions

Adopting VSCF to vibrations in solids requires the modeling of the extended system with a manageable number of atoms that are considered explicitly. This requires the choice of appropriate boundary conditions. One possible choice is to use free boundary conditions, surrounding the molecule with a few solvation layers and completely ignoring all effects due to atoms outside of this region. Such a simulation cell actually models the molecule embedded in a cluster rather than in a matrix, therefore its use is questionable in modeling the extended lattice environment. In fact, the differences in structure between the cluster and the solid can be appreciable enough to influence the medium effect on the spectrum. We found the following choices of boundary conditions to be most useful for the class of problems considered:

Periodic Boundary Condition: The most common technique to reduce finite-size effects is the use of periodic boundary conditions, common in the simulation of liquids and solids.[20] Because of the effective repetition of the system present in periodic calculations, an important requirement is that the range of interactions be smaller than half the size of the simulation box. This requirement is quite stringent in the present computations, as very accurate quadratic minima are needed to carry out vibrational analysis. In the present case, we found that using the common 108 atom cell to model an FCC lattice was not adequate, at least 256 atoms must be included. This, in turn, means that computations must be performed with as many as 765 coupled modes. Figure 1 shows the simulation cell and its periodic extension when Periodic Boundary Conditions are used.

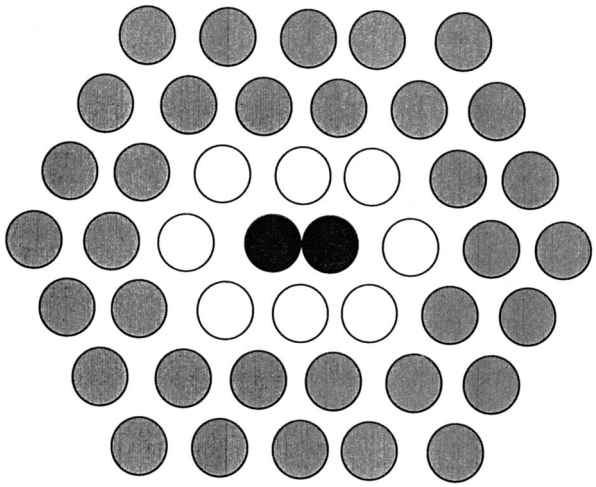

FIG. 2. Schematic picture of the Dynamical Cell with Rigid Walls boundary condition.

Dynamical Cell with Rigid Walls: The most useful boundary condition for the present application, one that retains accuracy and greatly reduces the computational overhead, is the one involving a few mobile layers around the molecule, surrounded by two more frozen solvation layers of the host lattice. We refer to this choice as a Dynamical Cell with Rigid Walls. In this treatment, the potential energy of a given configuration is calculated by taking all the atoms into account, but relaxation is only performed on the mobile layers. Also, vibrational modes are calculated only for the mobile part of the system. The effect of the frozen layers is to provide an external potential. The frozen layers that have the symmetry of the matrix and do not move during relaxation, ensure the proper structure of the lattice site for the molecule, and there are no unphysical rearrangements that would occur with free boundary conditions. On the other hand, the presence of mobile layers allows for dynamical simulation of the solid environment, delocalization of molecular modes and coupling between molecular and lattice vibrations are treated explicitly. In the specific case to be considered here, I_2 molecule isolated in an FCC lattice of argon atoms, we found that four solvation layers (448 atoms) with two layers (72 atoms) being mobile was sufficient for converged results. The computational efficiency of the applied scheme stems from the fact that, although the overall number of atoms considered is quite large, the most expensive parts of the computation scale with the number of modes, i.e., with the number of mobile atoms. All of the results to be presented were obtained using Dynamical Cell with Rigid Walls boundary conditions, which is schematically illustrated in Fig. 2. Computations took only a few hours on a personal computer.

III. SYSTEM AND POTENTIALS

The system studied here is I_2 isolated in argon matrices, on which high resolution data is available.[9,11] Argon crystal-

lizes in an FCC lattice with lattice parameter $a_0=5.3$ Å. Geometric considerations suggest that iodine occupies a double-substitutional site in the matrix. This description of the substitutional site has been amply verified through prior simulations of time-resolved observables.[21] As described in the previous section, our simulation cell includes four solvation layers around the molecule. We assume that the potential of I_2 in Ar_n system is given as the sum of three terms:

$$U=U_{\mathrm{Ar}_n}+U_{\mathrm{I}_2}+U_{\mathrm{I}_2-\mathrm{Ar}_n}. \tag{8}$$

Calculations are obviously easier if an analytic fit to the potentials is available, and we shall attempt this for all interactions used. The interaction between argon atoms is modeled by pairwise-additive Lennard–Jones potentials:

$$U_{\mathrm{Ar}_n}=\sum_{i<j} V_{LJ}(r_{ij}), \tag{9}$$

with parameters $\sigma=3.40$ Å, $\epsilon=84\ \mathrm{cm}^{-1}$.[22,23] For the I_2 molecule, we use the Morse potential,

$$U_{\mathrm{I}_2}=D_e(1-e^{-\beta(r-r_e)})^2, \tag{10}$$

with parameters extracted from the well-established gas-phase spectroscopic data ($r_e=2.666$ Å, $\omega_e=214.57\ \mathrm{cm}^{-1}$ and $\omega_e x_e=0.627\ \mathrm{cm}^{-1}$, where x_e is the anharmonicity parameter[24]). Since we are interested in an accurate representation of the potential near its minimum, we use $D_e=\omega^2/(4\omega_e x_e)=18{,}357\ \mathrm{cm}^{-1}$, and $\beta=0.12177\omega_e(\mu/D_e)^{1/2}=1.536\ \mathrm{Å}^{-1}$. As D_e is fitted to spectroscopic data, this potential does not properly describe the dissociation limit of the molecule.

We describe the interaction between the iodine molecule and argon atoms as the sum of three-atom terms:

$$U_{\mathrm{I}_2-\mathrm{Ar}_n}=\sum_i U_{\mathrm{I}_2-\mathrm{Ar}(i)}, \tag{11}$$

where Ar(i) refers to the ith argon atom. Several experimentally motivated semi-empirical potentials have been proposed in the literature to describe the I_2-Ar interaction. Early attempts used a ''dumb-bell'' potential with isotropic atom–atom potentials[25]

$$U_{\mathrm{I}_2-\mathrm{Ar}}=V(r_1)+V(r_2), \tag{12}$$

where r_i is the distance between the argon atom and the ith atom of I_2. Subsequently, it was found that such a potential does not correctly describe the properties of the I_2-Ar cluster.[26] In particular, I_2-Ar has two distinct isomers, a linear and a T-shaped one,[27] with similar binding energies. Isotropic potentials with the form of Eq. (12), fail to describe the binding of the linear isomer. We thus use the form suggested by Naumkin *et al.*,[28] which employs anisotropic atom–atom potentials to describe the I_2-Ar interaction:

$$U_{\mathrm{I}_2-\mathrm{Ar}}=V(r_1,\phi_1)+V(r_2,\phi_2), \tag{13}$$

where $r_{1;2}$ are the I–Ar distances, and $\phi_{1;2}$ are the I–I–Ar angles between the I–Ar radius vectors and the I–I bond, and

$$V(r,\phi)=V_{\mathrm{L}}(r)\cos^2\phi+V_{\mathrm{P}}(r)\sin^2\phi, \tag{14}$$

TABLE I. Measured/*ab initio* values of I_2-Ar bond lengths, binding energies and harmonic frequencies for the T-shaped and for the linear complex, as reported in the literature.

Reference	R_T/ Å	U_T/ cm^{-1}	ω_T/ cm^{-1}	R_L/ Å	U_L/ cm^{-1}	ω_L/ cm^{-1}
30	4.02	250	27	…	…	…
31	4.16	179	24	5.16	193	27
33	3.87	265	26	5.09	250	28

where V_L and V_P correspond to the linear and perpendicular directions, with respect to the I–I bond. In this work, we used the Morse form for both V_L and V_P. This form of the potential is in the spirit of the DIM (Diatomic in Molecules) approach[29] that, for the I_2-rare gas case constructs the potential energy surface from anisotropic atom–atom potentials. We constructed three different I_2-Ar potentials, based on the values of the I_2-Ar bond lengths (measured from the center of the iodine molecule), the binding energies, and the harmonic frequencies around equilibrium for both of the T-shaped and for the linear configurations. In Table I, we list these quantities, as reported in the literature. Although the results of Levy *et al.*[30] only correspond to the T-shaped isomer, we include them here, since the isotropic potentials based on his data are still widely used. The other two sets present values that more or less bracket the reported range in the literature. The results of Kunz *et al.* are based on recent *ab initio* calculations,[31] and agree with the experimental findings of Klemperer *et al.*[32] Naumkin *et al.* calculated the potential energy surface with a scaled *ab initio* scheme.[33] Their results are close to the earlier potentials of Buchachenko *et al.*[34] who worked with the semi-empirical DIM scheme. The main difference between these two sets of values is that Naumkin *et al.* predict shorter bond-lengths and deeper minima for both isomers. We derived Morse parameters for all three sets. In the case of the results of Levy *et al.*, we assumed an isotropic form, i.e., we set the parameters corresponding to the perpendicular and parallel potentials equal. The resulting sets of Morse parameter values are summarized in Table II. The structure of the cage surrounding the I_2 molecule is shown in Fig. 3. The structures obtained with all three I_2-Ar potentials are very similar, but the differences still play a role in the magnitudes of the spectroscopic shifts.

IV. RESULTS AND DISCUSSION

To test the validity of our boundary condition in modeling the vibrational modes of the crystal, we first performed a harmonic analysis of the neat argon lattice using our simulation cell. The obtained, smoothed density of states, which is

TABLE II. Parameters of the Morse potentials in Eq. (14), constructed to reproduce different sets of values in Table I.

Model potential	r_e^P/Å	D_e^P/cm^{-1}	$\beta^P/\mathrm{Å}^{-1}$	r_e^L/Å	D_e^L/cm^{-1}	$\beta^L/\mathrm{Å}^{-1}$
Levy *et al.*	4.23	127	1.3	4.23	127	1.3
Kunz *et al.*	4.41	81	1.4	3.84	186	1.4
Naumkin *et al.*	4.14	123	1.25	3.78	234	1.25

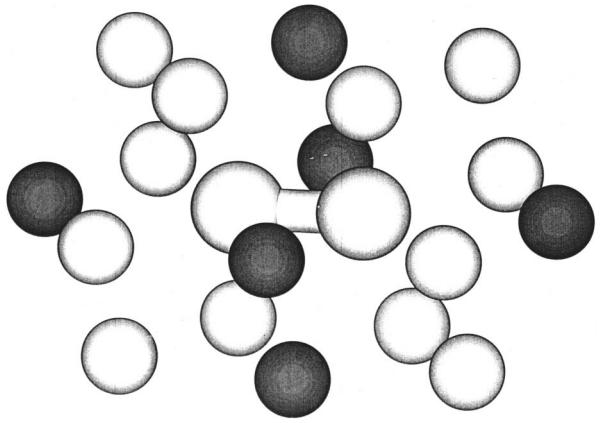

FIG. 3. Iodine molecule and the first solvation layer of argon atoms in the matrix. Shaded argon atoms correspond to T-shaped and linear I_2-Ar complexes.

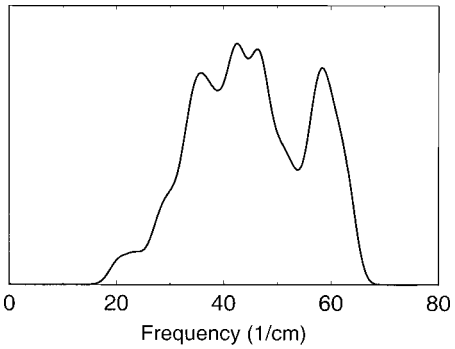

FIG. 4. Density of states calculated for argon, using simulation cell described in text.

plotted in Fig. 4, is in good agreement with the known phonon spectrum of solid argon.[35] The main difference is the absence of long-wavelength vibrations due to the limited size of the simulation cell. This is not a serious concern in the present application, since the impurity vibrations are strongly localized, and matrix shifts are predominantly determined by the short-wavelength modes which are well-described in our model.

To simulate the doped solid, we replace the central pair of nearest neighbor argon atoms with molecular iodine. The structure of the first solvation cell is shown on Fig. 3. Three separate calculations are performed using the three different sets of potential parameters described in the previous section. After allowing the simulation cell to relax to its minimum energy configuration, a harmonic analysis is performed to determine the normal modes and their frequencies. The normal modes are used to carry out the VSCF calculations, with only pair-wise mode-couplings taken into consideration. An 8-point grid is used for all lattice modes, except for the I–I stretch mode. For the latter, a 32-point grid was used to represent the vibrational wave-functions of the first 8 excited states with accuracy. Excited lattice modes were not considered. The calculation yields the excited state energies, from which the level spacings are obtained from the energy difference between successive vibrational states.

The harmonic frequencies are collected in Table III, together with experimental values for gas-phase and matrix-isolated iodine. The computed level spacings, $E_v - E_{v-1}$ versus v, are plotted in Fig. 5 for all three sets of potential parameters. The VSCF frequencies and anharmonicities reported in Table III are obtained from intercepts and slopes of the linear fits to the data. The VSCF frequencies are ca. 0.2 cm^{-1} lower than the harmonic ones, an effect that must be attributed to the anharmonic coupling between the molecule and lattice. Inspection of Table III shows that according to the experimental findings, the vibrational frequency of molecular iodine undergoes 1–1.5 cm^{-1} red shift upon solvation in solid argon. The calculated frequency shifts depend on the choice of potentials. The isotropic I–Ar potential, which was based on measurements by Levy *et al.*, yields a VSCF frequency blue shifted by 0.75 cm^{-1} (0.95 cm^{-1} in the harmonic analysis). The anisotropic potential fitted to the *ab initio* values calculated by Kunz *et al.* does not produce an appreciable matrix shift. The parametrization based on the potential by Naumkin *et al.* produces a red shift of 1.2 cm^{-1}, which is bracketed by the experimental values obtained from the two different measurements. Indeed, the agreement between experiment and theory is even better than what may be concluded from the comparison of extrapolated data. Resonance Raman spectroscopy directly measures transition frequencies. Time resolved CARS also measures level spacings directly, in the form of beat frequencies. Since the VSCF calculations yield excited state energies, we may directly compare the experimental points with the simulations. This is done in Fig. 5, where it can be seen that within the reported error bars, the experiment coincides with the simulations based on the anisotropic potentials of Naumkin *et al.*

It can be safely concluded that it is necessary to include the anisotropy of the I–Ar pair potential to describe the energetics in the matrix. Moreover, it seems that the anisotropic potential of Naumkin *et al.*,[33] when used in the three-body form of Eq. (13), yields a better agreement with experiment that the parametrization based on the potential by Kunz *et al.*[13] Such statements are only possible because the VSCF method yields the excited state energies with their anharmonicities and anharmonic couplings to the lattice modes, therefore allowing a direct and accurate simulation of the experimental observables.

TABLE III. Frequencies of I–I stretch obtained with harmonic analysis, and frequencies and anharmonicities obtained with VSCF, using different model potentials. Gas-phase and matrix-isolation experimental results are also shown. All frequencies in cm^{-1}.

Model potential	ω_{Har}	ω_{VSCF}	$(\omega_e x_e)_{\mathrm{VSCF}}$
Levy *et al.*	215.51	215.31	0.61
Kunz *et al.*	214.63	214.47	0.61
Naumkin *et al.*	213.70	213.39	0.62
Experiment	ω_e	$\omega_e x_e$	
Gas-phase (Ref. 24)	214.57	0.627	
RR in matrix (Ref. 9)	213.70	0.60	
CARS in matrix (Ref. 11)	213.05	0.57	

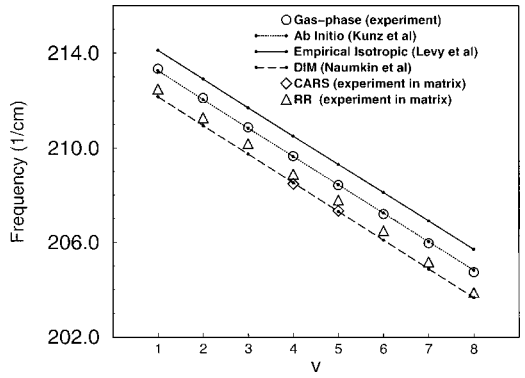

FIG. 5. Measured and computed anharmonic frequencies for the I–I stretch overtones in an argon matrix.

Given the success of the method in reproducing the experimental red shift, it is useful to analyze the origin of the matrix shifts that differ in magnitude and sign for the different model potentials. To this end, we investigate the equilibrium structure of the simulation cells. The immediate cage around the molecule shows small distortions that depend on the potential used. As a characteristic measure of the distortions, we calculated the I–Ar distances for the argon atoms in the ''T-ring'' and for the atoms collinear with the molecule (the shaded atoms on Fig. 3). We compare these distances to those in the ''T'' and in the linear isomers of the I_2-Ar complex. The differences $\Delta r = r^{\text{solid}} - r^{\text{complex}}$, together with the I–I bond lengths are given in Table IV. Inspection of Table IV shows that the argon ring around the iodine bond in the matrix is significantly tighter than in the triatomic complex. In contrast, the collinear I–Ar distances are longer than in the complex. In effect, the substitutional trapping site in argon produces a compressive stress in the plane perpendicular to the molecule and a tensile stress along the I–I axis. The strain of the molecular bond is correlated with the tensile stress, but not with the compressive stress. Thus, for the potential based on Levy *et al.*,[30] the difference in the collinear I–Ar distance between complex and solid is negligible; consistent with this, the iodine bond length remains the same as in the free molecule. As Δr_L increases in the anisotropic potentials, so does the tensile strain of the iodine bond. The observed matrix shifts are determined by a delicate balance between the compressive and tensile stresses. Thus, in the case of the potential based on Levy *et al.*, the observed blue shift must be entirely ascribed to the compressive stress perpendicular to the molecular axis. In the case of the Kunz *et al.* potential, since Δr_T is even smaller, the compressive stress is larger, and therefore, a larger blue shift would be expected. However, this is counter balanced by the tensile stress along the molecular axis, to render the matrix shift negligible. The potential by Naumkin *et al.*, featuring the shortest I–Ar equilibrium bond lengths in both directions, predicts the smallest compressive and the greatest tensile stress on the molecule. The combined effect is a red shift that is remarkably close to the experimental value. We may conclude that local cage structure and the associated matrix shift are sensitive functions of the I–Ar potential and its angular anisotropy.

TABLE IV. Difference between I–Ar distances for the argon atoms in the ''T'' and linear geometries in the solid and in the complex, and the length of the I–I bond after relaxation using different potentials.

Potential	Δr_T/Å	Δr_L/Å	r_{I_2}/Å
Levy *et al.*	−0.36	0.01	2.666
Kunz *et al.*	−0.45	0.27	2.668
Naumkin *et al.*	−0.31	0.36	2.669

To assess the dynamical contribution to the observed matrix shift, we performed a VSCF calculation in which the lattice atoms were frozen in their equilibrium geometry. The red shift for the I_2 vibration in the static field of the Ar atoms was about $0.3\ \text{cm}^{-1}$ smaller than in the previous case. This shows that the main part of the red shift is due to static effects described previously (cage structure); however a nonnegligible part is caused by coupling to the modes of the matrix. We may conclude that the explicit treatment of the lattice vibrations is necessary to accurately quantify matrix shifts.

V. CONCLUSIONS

In this paper we introduced an extension of the vibrational self-consistent field method for calculations of molecular vibrational spectroscopy in a crystalline solid environment. Calculations are done on a simulation cell in which the first two solvation shells are treated dynamically, while two additional layers are frozen.

Using the prototype of iodine isolated in an argon matrix, we demonstrated that the algorithm is a powerful tool for matrix spectroscopy. The matrix shifts are very small in this system. Our results show that the method, which can certainly be applied to large shifts, can also deal with very small effects when necessary. The method allows a direct calculation of energies of vibrationally excited states, and therefore, affords a direct comparison with experimental data. Moreover, the method allows the analysis of local structure and dynamics to establish the origins of matrix effects on spectroscopic observables. Finally, the reproduction of the red shift that is observed in this case allows the assessment of the various I_2-Ar potentials that have been suggested in the literature. Anisotropic I–Ar potentials are found to be essential for reproducing experimental results of matrix isolation spectroscopy. Potentials parametrized using the scaled *ab initio* potential by Naumkin *et al.*[33] yield almost perfect agreement with the experiments. Both static and dynamic contributions are accounted in the VSCF treatment, and both have been shown to play significant roles in this case.

Based on the results, many more applications are possible in the future. Due to the good scalability of our algorithm, quantitative spectroscopic calculations on substantially greater polyatomic molecules are feasible. Use of *ab initio* potentials for the molecule, together with empirical potentials to describe guest-host and host-host interactions, is also possible. It may be useful to treat other types of solid systems; we plan to adopt the method in the study of molecular crystals and for molecules adsorbed on surfaces.

ACKNOWLEDGMENTS

The authors thank Dr. Nicholas Wright and Professor Ken Janda for their helpful comments. The work at U.C. Irvine was supported by a grant of the MCB division of the Natural Science Foundation (Subcontract of MCB-9982629, to R.B.G.). The work at the Hebrew University was supported by the DFG, Germany, under project Sfb450.

[1] E. Whittel, D. A. Dows, and G. C. Pimentel, J. Chem. Phys. **22**, 1943 (1954).
[2] H. E. Hallam, *Vibrational Spectroscopy of Trapped Species* (Wiley, London, 1973).
[3] L. Andrews and M. Moskovits, *Chemistry and Physics of Matrix-isolated Species* (Elsevier, New York, 1989).
[4] V. E. Bondybey, A. M. Smith, and J. Agreiter, Chem. Rev. **96**, 2113 (1996).
[5] V. A. Apkarian and N. Schwentner, Chem. Rev. **99**, 1481 (1999).
[6] H. J. Jodl, in *Chemistry and Physics of Matrix-isolated Species*, edited by L. Andrews and M. Moskovits (Elsevier, New York, 1989).
[7] S. Califano, V. Schettino, and N. Neto, *Lattice Dynamics of Molecular Crystals* (Springer, New York, 1981).
[8] R. B. Gerber and J. O. Jung, *Computational Molecular Spectroscopy*, edited by P. R. Bunker and P. Jensen (Wiley, Sussex, U.K., 2000).
[9] W. F. Howard and L. Andrews, J. Raman Spectrosc. **2**, 442 (1974); J. Grzybowski and L. Andrews, J. Raman Spectrosc. **4**, 99 (1975).
[10] J. Almy, K. Kizer, R. Zadoyan, and V. A. Apkarian, J. Phys. Chem. A **104**, 3508 (2000).
[11] M. Karavitis, R. Zadoyan, and V. A. Apkarian, J. Chem. Phys. **114**, 4131 (2001).
[12] J. O. Jung and R. B. Gerber, J. Chem. Phys. **105**, 10332 (1996).
[13] S. K. Gregurick, E. Fredj, R. Elber, and R. B. Gerber, J. Phys. Chem. **B101**, 8595 (1997).
[14] S. K. Gregurick, J. H-Y. Lin, D. A. Brant, and R. B. Gerber, J. Phys. Chem. **B103**, 3476 (1999).
[15] G. M. Chaban, J. O. Jung, and R. B. Gerber, J. Chem. Phys. **111**, 1823 (1999).
[16] D. T. Colbert and W. H. Miller, J. Chem. Phys. **96**, 1982 (1992).
[17] N. J. Wright and R. B. Gerber, J. Chem. Phys. **112**, 2598 (2000).
[18] R. B. Gerber and M. A. Ratner, Chem. Phys. Lett. **68**, 195 (1979).
[19] A. E. Roitberg, R. B. Gerber, R. Elber, and M. A. Ratner, Science **268**, 1319 (1995).
[20] M. P. Allen and D. J. Tildesley, *Computer Simulation of Liquids* (Oxford University Press, New York, 1987).
[21] R. Zadoyan, J. Almy, and V. A. Apkarian, Faraday Discuss. **108**, 255 (1997), and references therein.
[22] C. Kittel, *Introduction to Solid State Physics* (Van Nostrand Reinhold, New York, 1950).
[23] R. A. Aziz, J. Chem. Phys. **99**, 4518 (1993).
[24] G. Herzberg, *Spectra of Diatomic Molecules* (Wiley, New York, 1976).
[25] R. E. Smalley, L. Wharton, and D. H. Levy, J. Chem. Phys. **68**, 671 (1978).
[26] A. Rohrbacher, N. Halberstadt, and K. C. Janda, Annu. Rev. Phys. Chem. **51**, 405 (2000).
[27] M. L. Burke and W. Klemperer, J. Chem. Phys. **98**, 1797 (1993).
[28] F. Y. Naumkin and P. J. Knowles, J. Chem. Phys. **103**, 3392 (1995).
[29] P. J. Kuntz, in *Theory of Chemical Reaction Dynamics*, edited by M. Baer (CRC, Boca Raton, 1985), Vol. I.
[30] J. A. Blazy, B. M. DeKoven, T. D. Russel, and D. H. Levy, J. Chem. Phys. **72**, 2439 (1980).
[31] C. F. Kunz, I. Burghardt, and B. A. Heb, J. Chem. Phys. **109**, 359 (1998).
[32] A. E. Stevens Miller, C. C. Chuang, H. C. Fu, K. J. Higgins, and W. Klemperer, J. Chem. Phys. **111**, 7844 (1999).
[33] F. Y. Naumkin and F. R. W. McCourt, Chem. Phys. Lett. **294**, 71 (1998).
[34] A. A. Buchachenko and N. F. Stepanov, J. Chem. Phys. **104**, 9913 (1996).
[35] S. S. Cohen and M. L. Klein, J. Chem. Phys. **61**, 3210 (1974).